

Supporting Information

Tetrazole-based energetic coordination compounds as enhanced catalysts for the thermal decomposition of ammonium perchlorate

Bo-Wen Fan,^{a,c,e} Meng Cui,^{c,e} Jing Qin,^d Jun Hu,^{a,c,e} Mei-Qing Lai,^{a,c,e} Jian-Gang Xu,^{*b,c,d} Fa-Kun Zheng,^{*c,e} Guo-Cong Guo^{c,e}

^a *College of Chemistry and Materials Science, Fujian Normal University, Fuzhou, Fujian 350007, P. R. China;*

^b *State Key Laboratory of Transient Chemical Effects and Control, Shaanxi Applied Physics and Chemistry Research Institute, Xian, Shaanxi, 710061, P. R. China;*

^c *State Key Laboratory of Structural Chemistry, Fujian Institute of Research on the Structure of Matter, Chinese Academy of Sciences, Fuzhou, Fujian 350002, P. R. China;*

^d *College of Material Engineering, Fujian Agriculture and Forestry University, Fuzhou, Fujian 350108, P. R. China;*

^e *Fujian College, University of Chinese Academy of Sciences, Beijing, 100049, P.R. China;*

* Corresponding authors: J.-G. Xu, jgxu@fafu.edu.cn; F.-K. Zheng, zfk@fjirsm.ac.cn; G.-C. Guo, gcguo@fjirsm.ac.cn

Index:

1. Experimental details	3
1.1 Safety precautions	3
1.2 Materials and Measurements	3
1.3 Synthesis of AP	4
1.4 Sensitivity test	4
1.5 Activation Energy Calculation	4
2. Tables	6
3. Graphics	9
4. References	12

1. Experimental details

1.1 Safety precautions

Compounds **1** and **2** pose significant hazards. Extreme caution must be exercised when handling these compounds. Protective measures, such as wearing gloves, protective glasses, and a leather apron, are essential. Moreover, these samples should be utilized in limited quantities. PETN is extremely hazardous and any step in the operation needs to be carried out under the necessary protective measures and standardized operation. The amount of synthesis must be controlled at the milligram level, and large quantities of synthesis are prohibited.

1.2 Materials and Measurements

All chemicals and solvents obtained from suppliers were used without further purification. All solvents were analytical grade reagent. $\text{Co}(\text{ClO}_4)_2 \cdot 6\text{H}_2\text{O}$ was from exploration platform. Single-crystal X-ray diffraction analysis was conducted on a Rigaku FR-X microfocus diffractometer employing graphite-monochromated Mo K_α radiation ($\lambda = 0.71073 \text{ \AA}$). The acquisition of crystal data was carried out using the ω -scan technique, and Lp effects were accounted for during data correction. The structures were initially solved using direct methods and subsequently refined using the full-matrix least-squares method based on F^2 , with anisotropic thermal parameters assigned to all non-hydrogen atoms. The positions of hydrogen atoms were determined *via* theoretical calculations and refined with consideration of an isotropic vibration factor. Powdered X-ray diffraction (PXRD) patterns were collected using a Rigaku Miniflex 600 diffractometer, employing Cu K_α radiation ($\lambda = 1.54184 \text{ \AA}$) at 15 mA and 40 kV in the 2θ range of $5\text{--}50^\circ$ and the simulated patterns were derived from Mercury Version 3.5 software. The elemental analyses of C, H, and N were conducted using an Elementar Vario EL III microanalyzer. FT-IR spectra were acquired using a Perkin-Elmer Spectrum instrument with KBr disks ranging from $4000\text{--}500 \text{ cm}^{-1}$. The thermal decomposition temperatures (T_{det}) of **1** and **2** were determined by a blast-proof DTA 552-Ex instrument manufactured by OZM Research (Czech Republic). The 5 mg sample was heated from $50 \text{ }^\circ\text{C}$ to $450 \text{ }^\circ\text{C}$ in a quartz tube at a rate of 10, 15, 20 $\text{K}\cdot\text{min}^{-1}$. The heat release test was carried out by TG-DSC NETZSCH STA 449F5 at a heating rate of $10 \text{ }^\circ\text{C min}^{-1}$. The SEM images were recorded on a Zeiss Sigma

300 field emission scanning electron microscope with the accelerating voltage of 2 kV. Solid-state UV-vis-NIR diffuse reflectance spectra were collected on UH4150 spectrophotometer using BaSO₄ as the reference. The sensitivities of the compounds were determined according to the BAM standard for friction and impact. The impact sensitivities were tested according to STANAG 4489 modified instruction using a BAM drop hammer. The friction sensitivities were tested according to STANAG 4487 modified instructions using a BAM friction tester.

1.3 Synthesis of AP

The synthesis of AP follows a currently well-established laboratory protocol. An aqueous solution containing 20ml of HClO₄ (70%) was added dropwise to an aqueous solution containing 20ml of NH₃·H₂O (22%) with high-speed stirring. The precipitate was obtained rapidly, and after filtration, washing and drying, pure AP was obtained.¹

1.4 Sensitivity test.

The sensitivities of the compounds were determined according to the BAM (German: Bundesanstalt für Materialforschung und Prüfung) standard for friction and impact. The classification of the tested compounds results from the ‘UN Recommendations on the Transport of Dangerous Goods’.

Impact sensitivity: The impact sensitivities of **1** and **2** were tested on a BAM fall hammer produced by OZM Research Impact sensitivity tests according to STANAG 4489. A 1 kg weight was dropped from a set height onto a 10 mg sample placed on a copper cap. The test results showed that the explosion happened with approximate 50% initiation probability. Impact sensitivities of **1** and **2** were observed to be 6.0 and 3.0 J, respectively.²

Friction sensitivity: The friction sensitivity was determined using a FSKM-10 BAM friction apparatus produced by OZM Research based on STANAG 4487. Friction sensitivities of **1** and **2** both were observed to be 72 and 48 N, respectively.⁵

1.5 Activation Energy Calculation

The apparent activation energy (E_a) was determined using the Kissinger equation:³⁻⁵

$$\ln(\beta/T_p^2) = \ln(AR/E_a) - E_a/(12 \times T_p)$$

β : Heating rate, $\text{K}\cdot\text{min}^{-1}$;

T_p : Characteristic peak temperature, K;

E_a : Apparent activation energy, $\text{J}\cdot\text{mol}^{-1}$;

A : Prefactor;

R : Universal gas constant, ($R = 8.314 \text{ J}\cdot\text{mol}^{-1}\cdot\text{K}^{-1}$)

2. Tables

Table S1. Crystal data and structure refinement for 1 and 2.

Compound	1	2
<i>CCDC</i>	2517391	2517392
<i>Empirical formula</i>	C ₁₂ H ₃₀ Cl ₂ CoN ₃₀ O ₈	C ₈ H ₂₄ Cl ₂ CoN ₂₀ O ₁₀
<i>M_r (g mol⁻¹)</i>	852.49	690.30
<i>Crystal system</i>	trigonal	monoclinic
<i>Space group</i>	<i>P</i> -3 (147)	<i>P</i> 2 ₁ / <i>c</i> (14)
<i>Z</i>	1	2
<i>a/Å</i>	11.9655(4)	8.4564(3)
<i>b/Å</i>	11.9655(4)	10.8285(3)
<i>c/Å</i>	6.8101(2)	13.8488(5)
<i>α/°</i>	90	90
<i>β/°</i>	90	100.029(3)
<i>γ/°</i>	120	90
<i>V/Å³</i>	844.40(6)	1248.75(7)
<i>D_c/g cm⁻³</i>	1.676	1.836
<i>Temperature (K)</i>	99.99(10)	99.97(10)
<i>F(000)</i>	437	706
<i>GOF on F²</i>	1.060	1.059
<i>R₁(I > 2σ(I))^a</i>	0.0556	0.0299
<i>wR₂(I > 2σ(I))^b</i>	0.1328	0.0746
<i>R₁(all data)^a</i>	0.0600	0.0342
<i>wR₂(all data)^b</i>	0.1361	0.0770

^a $R_1 = \sum(F_o - F_c)/\sum F_o$; ^b $wR_2 = [\sum w(F_o^2 - F_c^2)^2/\sum w(F_o^2)^2]^{1/2}$

Table S2. Selected bond distances (Å) and bond angles (°) for 1 and 2.

Compound 1			
Co1–N11	2.176(2)	Co1–N11#3	2.176(2)
Co1–N11#1	2.176(2)	Co1–N11#4	2.176(2)
Co1–N11#2	2.176(2)	Co1–N11#5	2.176(2)
N11#1–Co1–N11#2	91.58(8)	N11#1–Co1–N11#3	91.58(8)
N11#3–Co1–N11#4	180.00(10)	N11#1–Co1–N11	180.00
N11#3–Co1–N11	88.42(8)	N11#2–Co1–N11#3	91.58(8)
N11#1–Co1–N11#5	88.42(8)	N11#5–Co1–N11	91.58(8)
N11#2–Co1–N11	88.42(8)	N11#5–Co1–N11#3	88.42(8)
N11#2–Co1–N11#5	180.00(10)	N11#4–Co1–N11	91.58(8)
N11#2–Co1–N11#4	88.42(8)	N11#1–Co1–N11#4	88.42(8)
N11#5–Co1–N11#4	91.58(8)		
Compound 2			
Co1–O31#1	2.1557(11)	Co1–N11	2.1073(14)
Co1–O31	2.1557(11)	Co1–N21#1	2.1470(14)
Co1–N11#1	2.1072(14)	Co1–N21	2.1470(14)
O31–Co1–O31#1	180.0	N11–Co1–N21#1	91.05(5)
N11#1–Co1–O31	92.07(5)	N11–Co1–N21	88.95(5)
N11#1–Co1–O31#1	87.93(5)	N11#1–Co1–N21	91.05(5)
N11–Co1–O31#1	92.07(5)	N21#1–Co1–O31#1	90.79(5)
N11–Co1–O31	87.93(5)	N21#1–Co1–O31	89.22(5)
N11#1–Co1–N11	180.0	N21–Co1–O31	90.78(5)
N11#1–Co1–N21#1	88.95(5)	N21–Co1–O31#1	89.21(5)
N21#1–Co1–N21	180.00(4)		

Symmetry codes for **1**, #1: $2 - x, -y, 1 - z$; #2: $1 + y, 1 - x + y, 1 - z$; #3: $+x - y, -1 + x, 1 - z$; #4: $2 - x + y, 1 - x, +z$; #5: $1 - y, -1 + x - y, +z$.

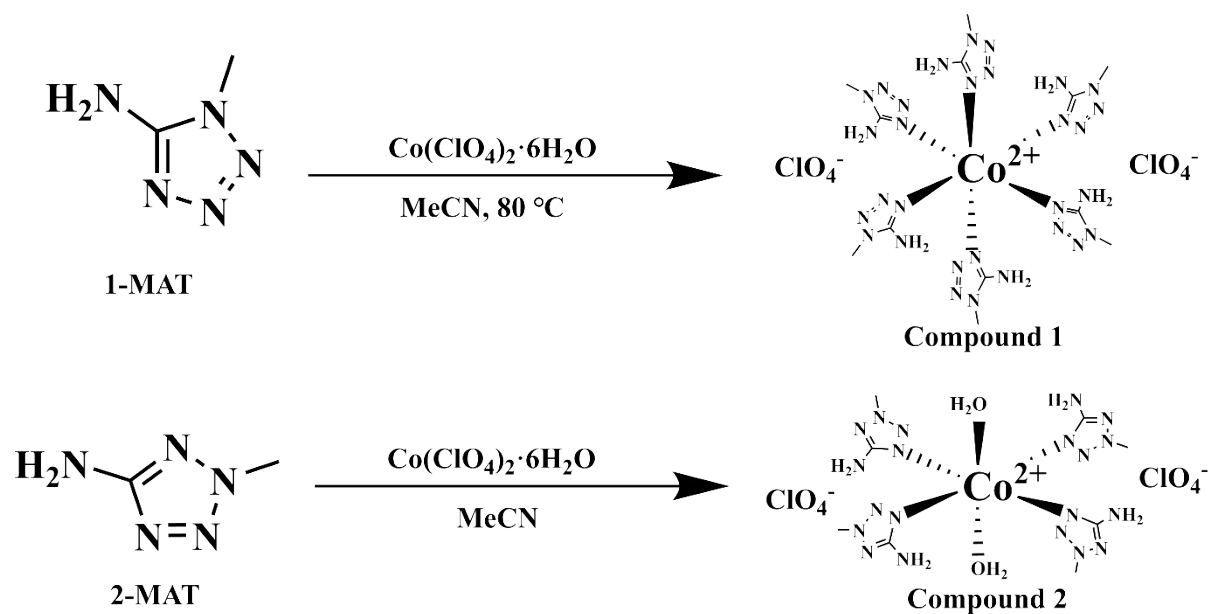
Symmetry codes for **2**, #1: $1 - x, 1 - y, 1 - z$.

Table S3. Performance Characterization of Similar Compounds.

Compound	T_{exo}^a (°C)	HTD ^b (°C)	IS ^c (J)	FS ^d (N)
Compound 1	230.6	245.2	6	72
Compound 2	198.8	234.3	3	48
[Cu(1-PryTz) ₆](ClO ₄) ₂ ⁶	135	-	2	5
[Fe(1-PryTz) ₆](ClO ₄) ₂ ⁶	168	-	2	6
[Zn(1-PryTz) ₆](ClO ₄) ₂ ⁶	164	-	2	15

^a Onset of exothermic event in the DTA; ^b High-temperature decomposition; ^c Impact sensitivity; ^d Friction sensitivity.

3. Graphics



Scheme S1. Synthetic routes for **1** and **2**.

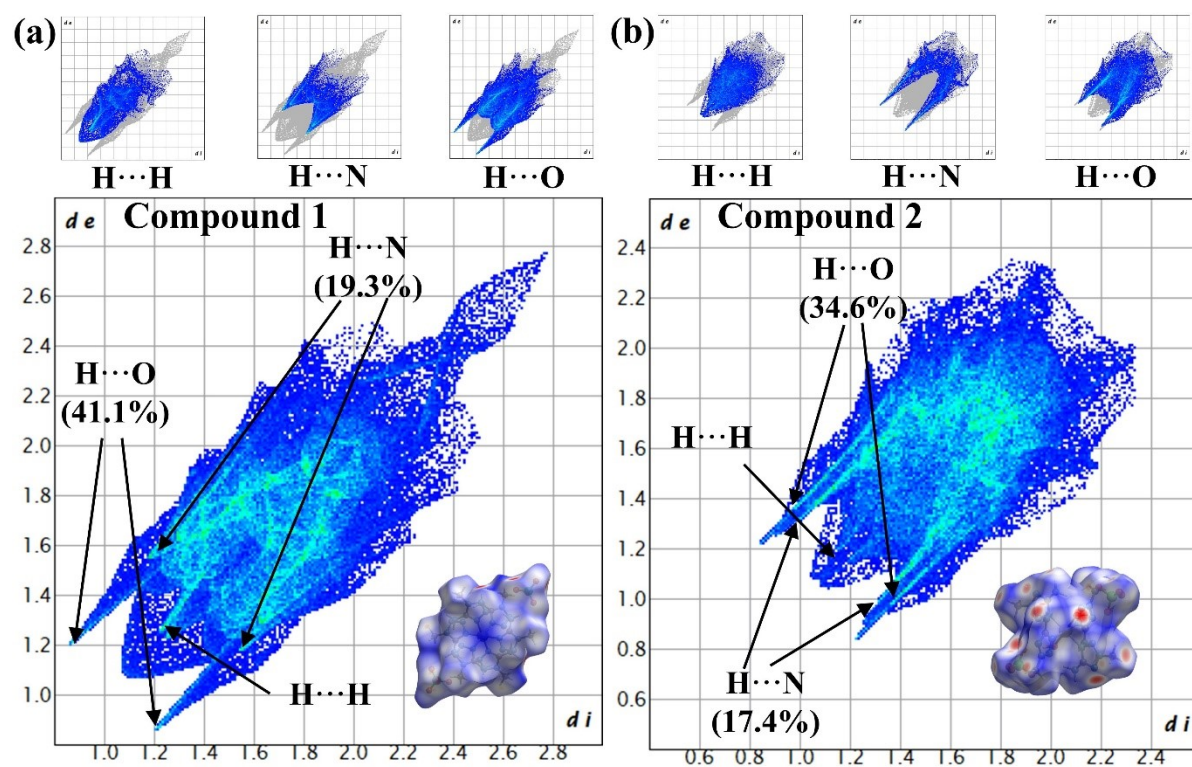


Figure S1. Hirshfeld surface and Fingerprint plots of **1** (a) and **2** (b), with A...B indicating atoms within and outside the Hirshfeld surface.⁷

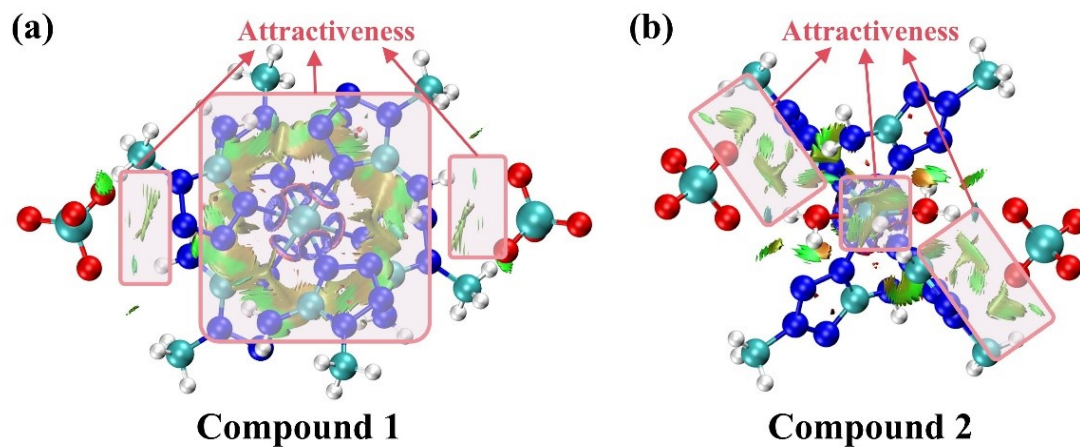


Figure S2. The weak interactions of 1 (a) and 2 (b).

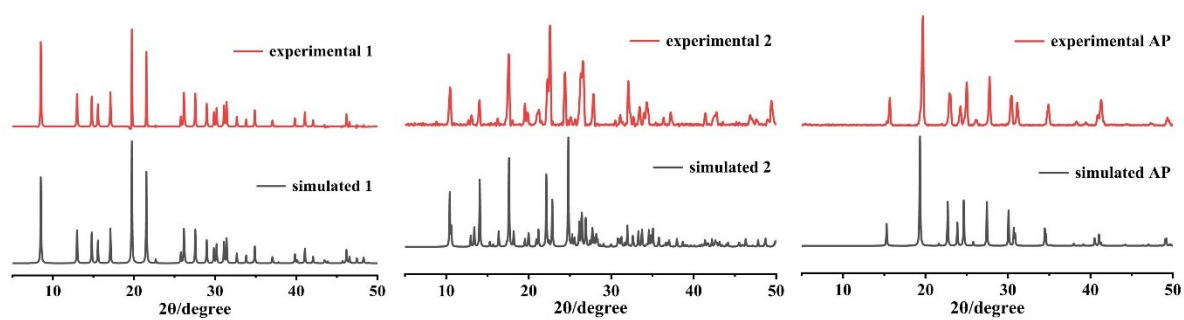


Figure S3. The stability tests on 1, 2 and AP.

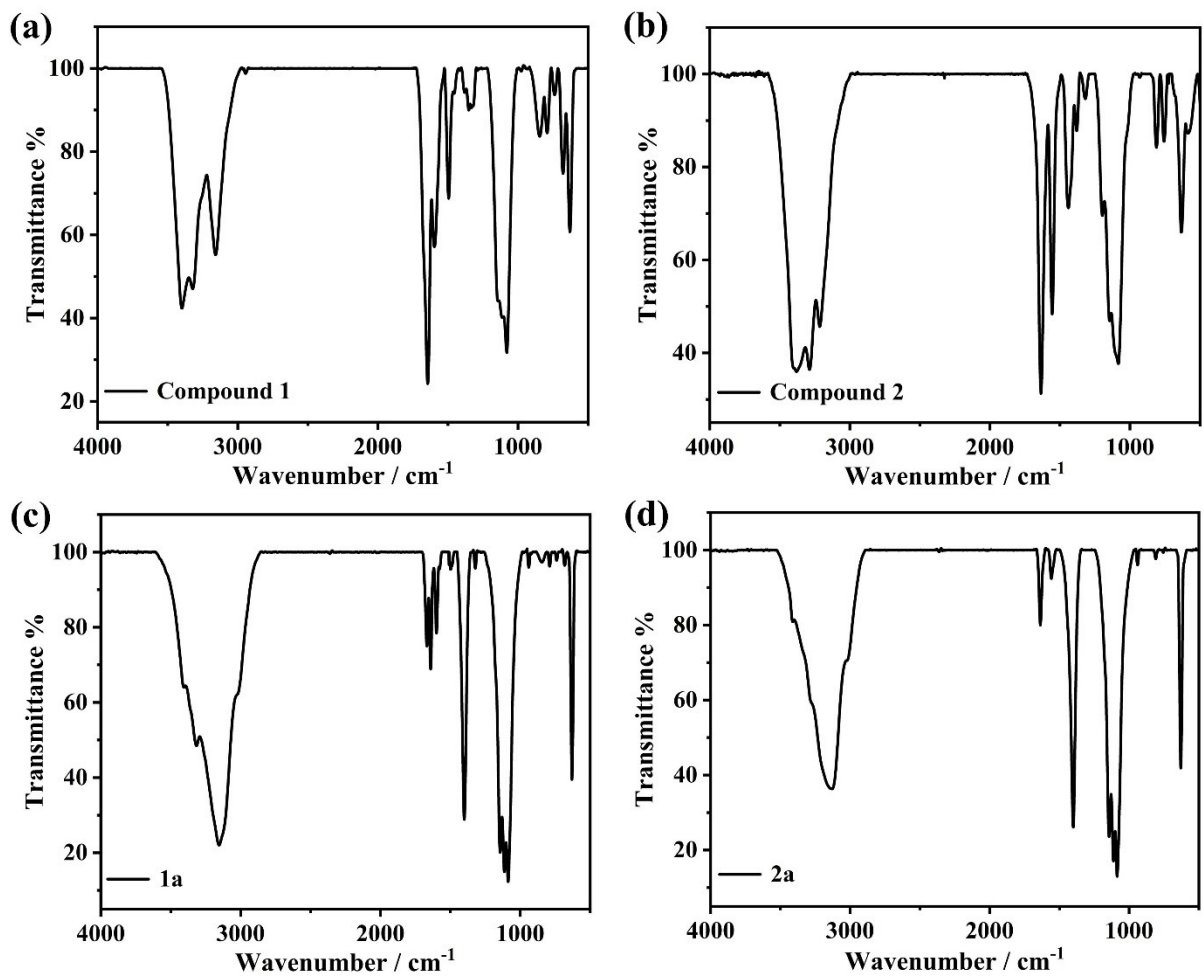


Figure S4. The IR spectra of **1** (a), **2** (b), **1a** (c) and **2a** (d).

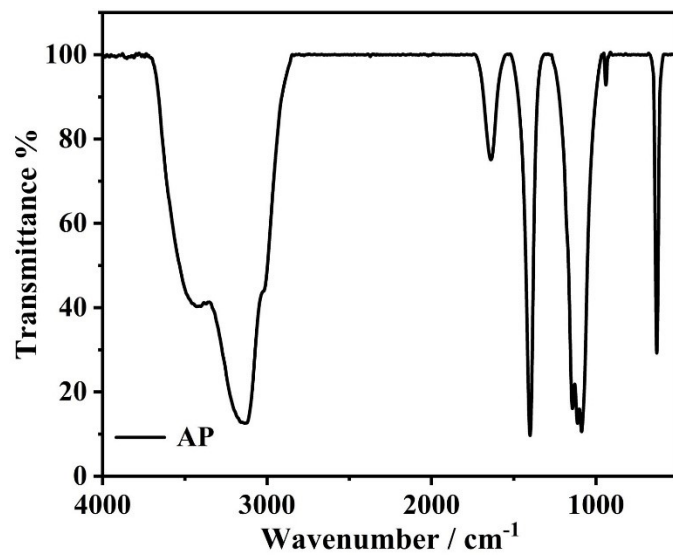


Figure S5. The IR spectra of AP.

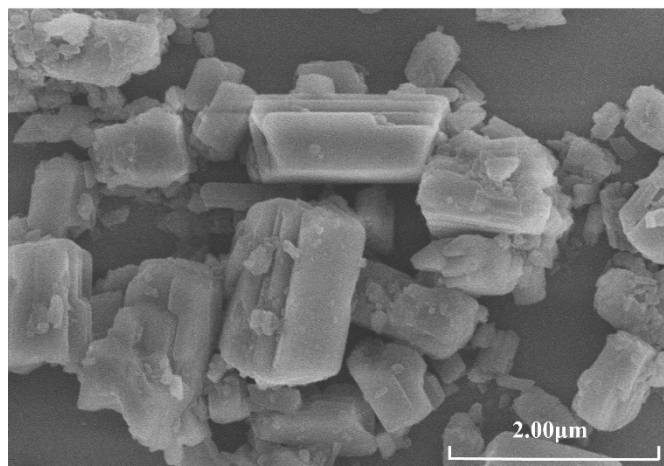


Figure S6. The SEM results of AP.

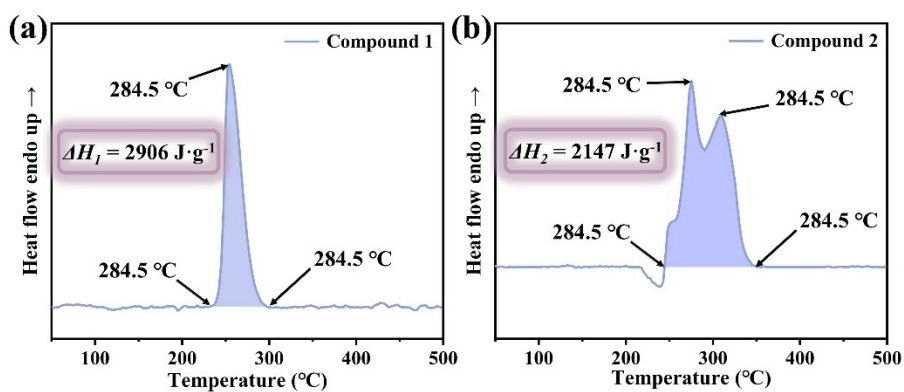


Figure S7. The DSC curves and heat release amounts of 1 (a) and 2 (b).

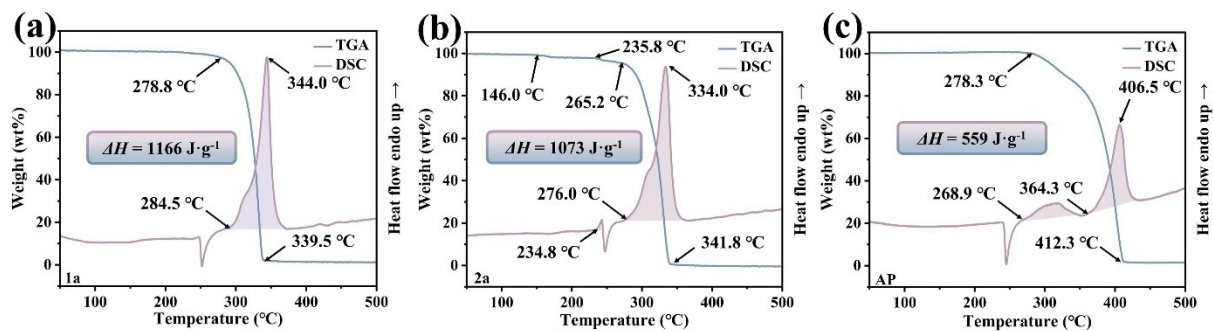


Figure S8. DSC and TGA curves of 1a (a), 2a (b) and AP (c).

4. References

1. M. Zhang, S. Wang, X. Y. Wang, Z. P. Wu, B. S. Ding, L. Yang, W. C. Tong, Q. Ma and Q. Y. Wang, *Adv. Sci.*, 2025, **12**, e01761.
2. Impact: insensitive > 40 J, less sensitive ≥ 35 J, sensitive ≥ 4 J, very sensitive ≤ 3 J; Friction: insensitive > 360 N, less sensitive = 360 N, $80 \text{ N} < \text{sensitive} < 360 \text{ N}$, very sensitive ≤ 80 N, extremely sensitive ≤ 10 N.
3. W. S. Dong, P. P. Zhang, M. Q. Xu, Z. J. Lu, Z. M. Li, K. Wang, Q. Y. Yu and J. G. Zhang, *Small*, 2025, **21**, 2411382.
4. K. Li, J. Liao, S. Huang, Y. Lei, Y. Zhang and W. Zhu, *Inorg. Chem. Front.*, 2021, **8**, 4864–4877.
5. P. Zhou, S. Zhang, Z. Ren, X. Tang, K. Zhang, R. Zhou, D. Wu, J. Liao, Y. Zhang and C. Huang, *Adv. Sci.*, 2022, **9**, 2204109.
6. S. M. J. Endraß, T. M. Klapötke, J. T. Lechner and J. Stierstorfer, *FirePhysChem*, 2023, **3**, 330–338.
7. Z. Zhang, J. Liu, C. Mao, Y. Dong, M. Li, M. Tang, Y. Liu, G. Cheng, W. Huang and Y. Tang, *FirePhysChem*, 2025, DOI: 10.1016/j.fpc.2025.09.007.